Stable Transitions from Free-space to Contact: A Dynamical System Based Approach

Seyed Sina Mirrazavi Salehian* and Aude Billard

Abstract—In this work, we propose a dynamical system based strategy for establishing a stable contact with convex shaped surfaces during non-contact/contact scenarios. A contact is called stable if the impact occurs only once and the robot remains in contact with the surface after the impact. Realizing a stable contact is particularly challenging as the contact leaves a very short time-window for the robot to react properly to the impact force. In this paper, we propose a strategy consisting of locally modulating the robot's motion in a way that it aligns with the surface before making the contact. We show theoretically and empirically that by using the modulation framework, the contact is stable and the robot stays in contact with the surface after the first impact.

I. INTRODUCTION

In this short paper, we propose a control architecture to move fluidly from free-space-motions to motions in contact. Achieving a stable contact is the main focus of the paper which is particularly challenging as the contact leaves infinitesimal time for the robot to react properly to the impact forces. It is, however, necessary to establish a stable contact in many applications, e.g. wiping a table, dough rolling or polishing workpieces, to avoid that the robot bounces on the surface and damages itself or the environment.

The complexity of the problem increases importantly if the arm and the surface do not dissipate the impact energy; i.e perfectly elastic impact. In this case, to successfully establish a contact with a rigid surface, the robot should touch the surface with zero velocity so that the post-contact velocity in the normal direction is zero. Nevertheless, the impacts in real-world scenarios are mainly inelastic and the post-contact velocity of an object is a constant fraction of the pre-contact velocity [1]. In this case, touching the surface with zero, or near to zero, velocity results in a zero post-contact velocity in the normal direction; i.e., the robot remains in contact after the impact [2].

In this paper, by leveraging the properties of Dynamical Systems (DS) for immediate re-planning and their inherent robustness to real-time perturbations, we propose a strategy consisting of locally modulating a DS in the vicinity of the contact surface such that the direction and amplitude of the velocity is aligned with the surface; i.e., the velocity normal to the surface is canceled at the contact, see Fig.1. The proposed architecture can be integrated into existing DS-based motion control approaches, where they represent the nominal arm behavior.

All authors are with the School of Engineering, Ecole Polytechnique Federale de Lausanne (EPFL), Switzerland. {sina.mirrazavi;aude.billard}@epfl.ch
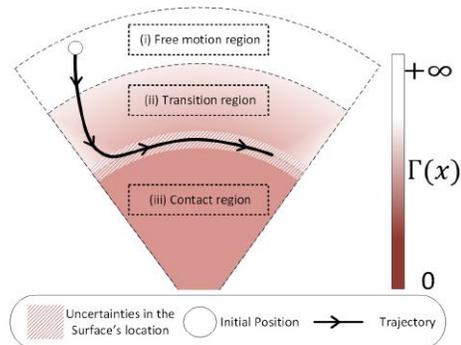*Corresponding author.

Fig. 1: Schematic of three subtasks in a non-contact/contact scenario. The arm starts approaching the surface at the *free motion* region. Once it is close enough to the surface, its velocity is regulated to establish a stable contact.

II. RELATED WORK

As well documented in the robotic/control literature, many different control architectures have been proposed for handling a physical contact. These architectures can be broadly categorized into two types. (i) direct or (ii) indirect force controllers. In the former category, the position and force controllers simultaneously govern the robot along unconstrained and constrained directions, respectively. On the same track, [3]–[6] proposed a hybrid control architecture in which a stable contact can be ultimately established after a finite number of bounces. [2], [7] proposed three control laws for the three motion regions. Once the first impact has occurred, the controller at the *transition* region is activated which, asymptotically, reduces the normal velocity to zero. In [8], an integral force compensation with a velocity feedback controller is proposed for force tracking and rejecting the effect of impacts, where the force regulation is activated once the impact is detected by the force sensor.

Indirect force control architectures, such as impedance controllers [9], [10] [32] or energy tank based architectures [11], [12], address the problem of switching between controllers by ensuring the desired contact force through compliant behavior to the end-effector. In [13], [14], a hybrid impedance(admittance)/time-delayed controller is proposed to absorb the impact force. Even though in the aforementioned works, it can be proved that the robot's motion and the contact is asymptotically/ultimately stable, there is no guarantee that the robot does not bounce on the surface after the first impact.

In our previous work [15], we proposed a control strategy for modulating the robots motion in such a way that a stable contact with flat and planar surfaces can be established. In this paper, we extend the control architecture in [15] to reach and stably enter into the contact with convex shaped surfaces.

III. PROBLEM STATEMENT

Suppose the contact surface is non-penetrable and passive. Moreover, a C^∞ function $(\Gamma(x) : \mathbb{R}^d \to \mathbb{R})$, which conveys a notion of distance to the surface, is available. We assume that the surface and the level curves of Γ enclose a convex region and this function monotonically increases with respect to the shortest distance between x and the surface. Hence, $\Gamma(x) = 0$ if and only if x is on the contact surface. Moreover, $\|\nabla\Gamma(x)\| \neq 0 \ \forall x \in \mathbb{R}^d$. Based on this definition, one can categorize the task space into three regions; namely the free-space region when $\rho < \Gamma(x)$, the transition region when $0 < \Gamma(x) < \rho$ and the contact region when $\Gamma(x) \leq 0$, see Fig.1, where $\rho \in \mathbb{R}^+$. We consider a class of continuous-time system given by the following model.

$$\ddot{x} = \mathsf{M}(x,\dot{x})f(x,\dot{x},t) \tag{1}$$

where $f(x,\dot{x},t)$ represents the nominal dynamical system which generates the nominal arm behavior. We assume that the nominal acceleration is non-zero in the contact and the transition regions; i.e. $f^T(x,\dot{x})f(x,\dot{x}) \neq 0 \ \forall(x,\dot{x}) = \mathbb{R}^{d\times d}|0 \leq \Gamma(x) < \rho$. $\mathsf{M}(x,\dot{x}) \in \mathbb{R}^{d\times d}$ is the modulation function which reshapes the nominal DS in such a way that it complies with the contact surface based on the state of the robot. We define the modulation function as follows:

$$\mathsf{M}(x,\dot{x}) = Q\Lambda Q^T \quad Q = \begin{bmatrix} q_1(x) & \dots & q_d(x) \end{bmatrix} \tag{2}$$

Where $q_i(x) \in \mathbb{R}^d \ \forall i \in \{1,\dots,d\}$ are orthonormal basis in $\mathbb{R}^d$ with $q_1(x)$ pointing in the normal of the surface; i.e. $q_1(x) = \frac{\nabla\Gamma(x)}{\|\nabla\Gamma(x)\|}$. $\boldsymbol{\lambda}_{ij}(x,\dot{x}) \ \forall i,j \in \{1,\dots,d\}$ are the entries of Λ, where i is the row number and j is the column number. To avoid undesirable modulations beyond the transition region, we limit the influence of the modulation function to the transition region:

$$\boldsymbol{\lambda}_{ij}(x,\dot{x}) = \begin{cases} \lambda_{ij}(x,\dot{x}) & \text{if } i=1, \ \Gamma(x) \leq \rho \\ \left(\lambda_{ij}(x,\dot{x}) - 1\right)e^{\frac{\rho-\Gamma(x)}{\varepsilon}} + 1 & \text{if } i=1, \ j=1, \ \rho < \Gamma(x) \\ \lambda_{ij}(x,\dot{x})e^{\frac{\rho-\Gamma(x)}{\varepsilon}} & \text{if } i=1, \ j\neq 1, \ \rho < \Gamma(x) \\ 1 & \text{if } i\neq 1, i=j \\ 0 & \text{if } i\neq 1, i\neq j \end{cases} \tag{3}$$

$\forall i,j \in \{1,\dots,d\}$, where $0 < \sigma$ defines the speed at which the modulation vanishes in the free-space region. ρ defines the region of the influence of the modulation function. If $\rho < \Gamma(x)$, $\Lambda = I_{d\times d}$. Hence. the robot is driven solely by the nominal dynamical system.

IV. COMPLIANT MODULATION FUNCTION

A. The elastic impact

Consider a scenario where the impact is perfectly elastic. In this case, to achieve a stable contact, the normal velocity[1] of the robot at the contact must be zero. To achieve this, we propose the following theorem

---

[1] For sake of simplify, in the rest of the paper, we call the velocity normal to the surface, the normal velocity.

Theorem 1: For a given initial state $\{x_0,\dot{x}_0 \in \mathbb{R}^d| \ 0 < \Gamma(x_0) \leq \rho, f(x_0, \ \dot{x}_0) \neq 0\}$, the motion generated by (1) and (2) makes contact with the surface with zero normal velocity, if $\forall j \in \{1,\dots,d\}$

$$\lambda_{1j}(x,\dot{x}) = \left(-\dot{x}^T \nabla q_1(x)^T \dot{x} - 2\omega q_1(x)^T \dot{x} - \omega^2\Gamma(x)\right)\mathbf{f}_j(x,\dot{x},t) \tag{4}$$

where $\mathbf{f}_j(x,\dot{x}) = \frac{f(x,\dot{x},t)^T q_j}{f(x,\dot{x},t)^T f(x,\dot{x},t)}$ and

$$\frac{|q_1(x_0)^T \dot{x}_0|}{\Gamma(x_0)} \leq \omega \tag{5}$$

Proof: see Appendix A.

If the robot starts its motion outside of the transition region, Eq. (3) states that the modulation function is activated once it enters the region. Hence, $(q_1^T x_0) = \rho$. In our previous work [15], we proposed a criterion to estimate the open parameters, namely ρ, ω, with respect to the robot's kinematic constraints.

B. The inelastic impact

In an inelastic impact, due to internal friction, the impact energy is dissipated. Hence, we can assume that if the normal velocity of the robot is very small $(-1 \ll \delta_{\dot{x}} \leq 0)$ on contact, the surface absorbs all the impact energy, i.e. the end-effector remains in contact after the impact [2]. We leverage this property and propose the following theorem:

Theorem 2: Assuming the impact is inelastic. For a given initial state $\{x_0,\dot{x}_0 \in \mathbb{R}^d| \ 0 < \Gamma(x_0) \leq \rho, \ f(x_0,\dot{x}_0) \neq 0\}$, the dynamical system (1) and (2) stably contacts the surface, if $\lambda_{1j}(x,\dot{x}) =$

$$\begin{cases} \left(-\dot{x}^T \nabla q_1(x)^T \dot{x} + \omega\left(-q_1(x)^T \dot{x} + (\delta_{\dot{x}}+v)\right)\right)\mathbf{f}_j(x,\dot{x}) & q_1^T \dot{x} < \delta_{\dot{x}} \quad (6) \\ \left(-\dot{x}^T \nabla q_1(x)^T \dot{x} + \omega\left(\frac{v}{\delta_{\dot{x}}}q_1^T \dot{x} - \omega(1-\frac{q_1^T \dot{x}}{\delta_{\dot{x}}})\Gamma(x)\right)\right)\mathbf{f}_j(x,\dot{x}) & \delta_{\dot{x}} \leq q_1^T \dot{x} \leq 0 \quad (7) \\ \left(-\dot{x}^T \nabla q_1(x)^T \dot{x} - 2\omega q_1(x)^T \dot{x} - \omega^2\Gamma(x)\right)\mathbf{f}_j(x,\dot{x}) & 0 < q_1^T \dot{x} \quad (8) \end{cases}$$

where

$$\frac{\delta_{\dot{x}} - q_1^T \dot{x}_0}{e^1 - 1} < v \tag{9}$$

, $\mathbf{f}_j(x,\dot{x}) = \frac{f(x,\dot{x},t)^T q_j}{f(x,\dot{x},t)^T f(x,\dot{x},t)}$ and $\frac{|q_1(x_0)^T \dot{x}_0|}{\Gamma(x_0)} \leq \omega$.

Proof: see Appendix B.

Till now, we have assumed that the distance between the robot and the surface can be accurately represented by $\Gamma(x)$. However, this might not be true in practice as noises might affect this value. To address this problem, the following proposition is presented:

Proposition 1: We assume a convex shaped surface with equation $\Gamma(x) + \eta$. η is the uncertainty in the surface's location, which is bounded with a known upper bound $\boldsymbol{\eta}$, i.e. $|\eta| \leq \boldsymbol{\eta} < \rho$. Moreover, for a given initial state $\{x_0,\dot{x}_0 \in \mathbb{R}^d| \ q_1^T \dot{x}_0 < \delta_{\dot{x}} < 0, 0 \leq \boldsymbol{\eta} < \Gamma(x_0) \leq \rho\}$, the dynamics of the robot is generated by the nominal DS (1) modulated by (2), where $\lambda_{1j}(x,\dot{x})$, $\forall(j) \in \{1,2,\dots,d\}$ are defined by (6). Then, the robot's normal velocity at the impact is bounded

TABLE I: The details of the systematic assessment. "Pre-contact" and "Pre-transition" velocities are the velocity of the end-effector in the normal direction when entering the *contact* and *transition* regions, respectively.

	Metallic surface and plastic tool	Metallic surface and tool
Pre-contact velocity	0.008 ± 0.006	0.006 ± 0.00
Pre-transition velocity	0.25 ± 0.13	0.28 ± 0.03

and the contact is stable, if ν and ω are defined as follows:

$$\nu = -\delta_{\dot{x}}, \quad \omega = \frac{\delta_{\dot{x}} - q_1^T \dot{x}_0}{\Gamma(x_0) - \boldsymbol{\eta}} \tag{10}$$

Proof: see Appendix C.

V. SIMULATION AND EXPERIMENTS

A. Simulation

The performance of the proposed framework is systematically evaluated in four different set of 2D simulations where the contact surface is defined as a circle, an ellipsoid and an oval. The nominal dynamic is defined by a critically damped second order dynamical system as follows, $f(x, \dot{x}) = -2K\dot{x} - K^2(x - x^*)$. x^* is the desired target. K is the rate of convergence learned from a set of demonstrations [16].

Qualitative and quantitative results are presented in Fig.4. Results from qualitative evaluation indicate that if the robot enters the transition phase, its motion is aligned with the surface and, hence, the contact is stable.

B. Empirical validation

We consider the task of wiping a planar and flat surface. The performance of the proposed framework is evaluated on a real robotic arm platform, i.e., 7 DOF robotic arm (KUKA IIWA). The robot is controlled at the level of joint positions at a rate of 200 Hz. The output of the DS (1) is converted into the joint state using the damped least squares inverse kinematic solver. The nominal DS is a second order dynamical system: $f(x, \dot{x}) = -40\dot{x} - \begin{bmatrix} 400 & 0 & 0 \\ 0 & 400 & 0 \\ 4000 & 4000 & 400 \end{bmatrix}(x - x^t)$. These values were chosen such that the robot enters the transition region. The surface of the object is approximated by a plane. The impact is assumed inelastic and $\delta_{\dot{x}} = -0.01 ms^{-1}$.

Two experimental set-ups are designed to assess the performance of the system. In the first one, both surface and the tool are metallic and rigid. In the second one, the surface is a metallic fender and the tool is made of plastic. Both scenarios were repeated 60 times for each set-up where the initial state of the robot is randomly chosen; all the information is summarized in Tab. I. The location of the surface is fixed. The snapshots of the motion execution in both experimental-set-ups are shown in Fig. 2 and Fig. 3. Visual inspection of video and the measurements confirms that, in all the trials, the robot stably makes contact with the surface. Nevertheless, the inspection of the measured velocity profiles indicates that in three cases the normal velocity at the impact is lower than $-0.01 ms^{-1}$. An example of the motion of the robot is illustrated in Fig. 3. As can be seen, the normal velocity of the robot is reduced to $\delta_{\dot{X}}$ in the *transition* region to ensure a stable contact.[2]

[2] A detailed experimental validation is presented in [15] and the videos available on-line here and here.
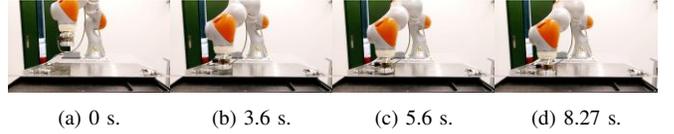

(a) 0 s.   (b) 3.6 s.   (c) 5.6 s.   (d) 8.27 s.

Fig. 2: Close-up snapshots of the end-effector motion. Both surface and the tool are metallic and rigid.
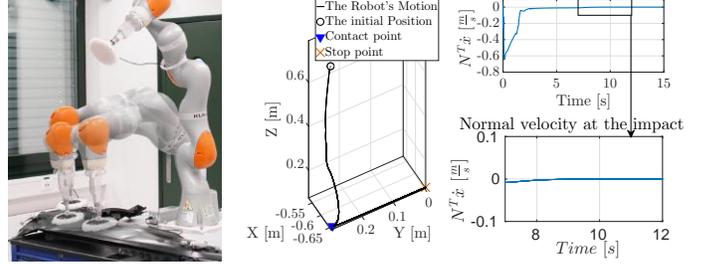

(a) Scenario 2   (b) Scenario 2

Fig. 3: The location of the surface is precisely measured. In the bottom right figures, the normal velocity of the robot at the impact region is illustrated.

VI. SUMMARY AND DISCUSSION

In this short paper, we propose a modulation strategy for controlling the robot's motion when making contact with a convex shaped surface. The core idea of the proposed approach is to reduce the robot's velocity to a certain threshold before entering into the contact with the surface such that the post-contact velocity becomes zero; i.e. the impact is stable and the robot does not bounce on the surface. The modulation strategy is proposed for both inelastic and elastic impacts. Even though the modulation function proposed for the inelastic impact is more complex than the elastic one, it can handle uncertainties related to the surface's location; i.e. Proposition 1. The source codes are available here and here. The video for planar simulations is available here.

In this paper, we have assumed that the object's surface is continuous and that we have an explicit function to describe the surface; i.e., $\Gamma(x)$. We have not explained how can obtain such a function. One way to address this problem is through approximating the contact surface through a convex hull [17] or regression methods; e.g., SVR [18].

We are currently working on an approach which benefits from the advantages of our modulation framework and hybrid force/position control architecture. In this way, the force-feedback information can be used not only for identifying the true location of the surface, but also for controlling the contact force while the robot slides on the surface.

APPENDIX

A. Proof of Theorem 1

As $q_i \, \forall i \in \{1, \ldots, D\}$ are the orthonormal basis in $\mathbb{R}^d$, $\forall w \in \mathbb{R}^d$, $w = \sum_{i=1}^{d} q_i(x)q_i(x)^T w$ and $\sum_{i=1}^{d} \nabla q_i(x)\dot{x}q_i(x)^T + q_i(x)\dot{x}^T \nabla q_i(x)^T = 0$. Hence, By substituting (4) and (2) into (1) and multiplying both side by $q_1^T(x)$:

$$q_1(x)^T \ddot{x} = q_1(x)^T Q \Lambda Q^{-1} f(x, \dot{x}, t) = \sum_{j=1}^{d} \lambda_{1j}(x, \dot{x}) q_j^T(x) f(x, \dot{x}, t)$$

$$= \frac{-\dot{x}^T \nabla q_1(x)^T \dot{x} - 2\omega q_1(x)^T \dot{x} - \omega^2 \Gamma(x)}{f(x, \dot{x}, t)^T f(x, \dot{x}, t)} f(x, \dot{x}, t)^T \sum_{j=1}^{d} q_j(x)q_j^T(x)f(x, \dot{x}, t) \tag{11}$$

$$= -\dot{x}^T \nabla q_1(x)^T \dot{x} - 2\omega q_1(x)^T \dot{x} - \omega^2 \Gamma(x)$$
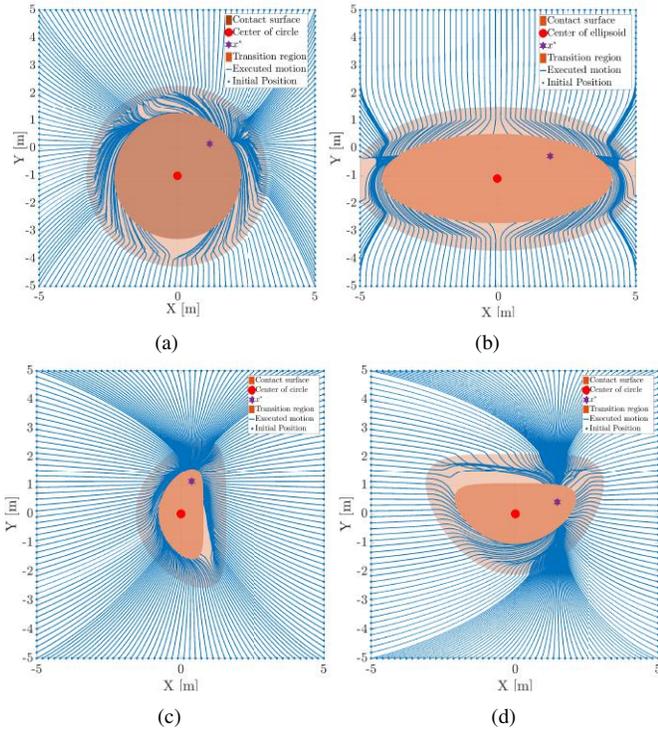
(a)

(b)

(c)

(d)

Fig. 4: $\delta_{\dot{x}} = -0.5$, $v = 0.05$. Contact in all the cases is stable. Among 200 trials, the lowest normal velocity at contact is $-0.47ms^{-1}$. As it can be seen, the motion is modulated such that it is aligned with the contact surface. The source code is available here.

Which is a critically-damped second order linear differential equation where ω defines the natural frequency of this system. The solution of (11) for a given initial state $\{\Gamma(x_0), q_1(x_0)^T \dot{x}_0\}$ is:

$$\Gamma(x) = e^{-t\omega}(\Gamma(x_0) + (\Gamma(x_0)\omega + q_1(x_0)^T \dot{x}_0)t) \tag{12}$$

Based on (5), as $\frac{|q_1(x_0)^T \dot{x}_0|}{\Gamma(x_0)} \leq \omega$ and $0 < \Gamma(x_0)$, $0 \leq \Gamma(x_0)\omega + q_1(x_0)^T \dot{x}_0$. Hence, $\lim_{t \to +\infty} \Gamma(x) = 0$. Moreover, $\lim_{t \to +\infty} q_1(x)^T \dot{x} = \lim_{t \to +\infty} e^{-t\omega}(q_1(x_0)^T \dot{x}_0 - (\Gamma(x_0)\omega + q_1(x_0)^T \dot{x}_0)\omega t) = 0$. Hence, the motion generated by (1) and (2) with respect to (4) and (5), enters the contact surface with zero normal velocity. Hence, the contact will be stable. ∎

B. Proof of Theorem 2

Substituting (6)-(8) and (2) into (1) and multiplying both sides by $q_1(x)^T$ yields: $q_1(x)^T \ddot{x} =$

$$\begin{cases} -\dot{x}^T \nabla q_1(x)^T \dot{x} - \omega\left(q_1(x)^T \dot{x} - (\delta_{\dot{x}} + v)\right) & q_1(x)^T \dot{x} < \delta_{\dot{x}} \tag{13} \\ \\ -\dot{x}^T \nabla q_1(x)^T \dot{x} + \frac{\omega^2 \Gamma(x) + v\omega}{\delta_{\dot{x}}} q_1(x)^T \dot{x} - \omega^2 \Gamma(x) & \delta_{\dot{x}} \leq q_1(x)^T \dot{x} \leq 0 \tag{14} \\ \\ -\dot{x}^T \nabla q_1(x)^T \dot{x} - 2\omega q_1(x)^T \dot{x} - \omega^2 \Gamma(x) & 0 < q_1(x)^T \dot{x} \tag{15} \end{cases}$$

It can easily be shown that $q_1(x)^T \ddot{x}$ defined by (13)-(15) is continuous. In the *third* region, $0 < q_1(x)^T \dot{x}_0$. Hence, $q_1(x)^T \ddot{x} = -\dot{x}^T \nabla q_1(x)^T \dot{x} - 2\omega q_1(x)^T \dot{x} - \omega^2 \Gamma(x)$, which is equal to (11). Therefore, as shown in Appendix A, the robot contacts the surface with zero normal velocity. In the *second* region, $\delta_{\dot{x}} \leq q_1(x)^T \dot{x} \leq 0$. Hence, $q_1(x)^T(x)\ddot{x} = -\dot{x}^T \nabla q_1(x)^T \dot{x} + \frac{\omega^2 q_1(x)^T x + v\omega}{\delta_{\dot{x}}} q_1(x)^T \dot{x} - \omega^2 q_1(x)^T x$. The aforementioned DS yields that if $q_1(x)^T \dot{x} = \delta_{\dot{x}}$, $\frac{dq_1(x)^T \dot{x}}{dt} = \omega v$ which is a positive value as $0 < \omega v$. Hence, one can conclude that if the robot enters the transition region, it does not cross the velocity boundary at $\delta_{\dot{x}}$; i.e. it does not get less than $\delta_{\dot{x}}$. Furthermore, if $0 < \Gamma(x)$ and $q_1(x)^T \dot{x} = 0$, $\frac{dq_1(x)^T \dot{x}}{dt} < 0$. Therefore, one can conclude that if the robot enters the transition region, it does not cross the velocity boundary at 0 as the normal acceleration at this state is negative. To sum up, in the *second* region, the robot moves towards the contact surface with the normal velocity between 0 and $\delta_{\dot{x}}$.

In the *first* region, $q_1(x)^T \dot{x}_0 < \delta_{\dot{x}}$. Hence, based on (13), $q_1(x)^T \ddot{x} = -\dot{x}^T \nabla q_1(x)^T \dot{x} - \omega\left(q_1(x)^T \dot{x} - (\delta_{\dot{x}} + v)\right)$. The solution of the aforementioned dynamic for a given initial state $\{\Gamma(x_0), q_1(x_0)^T \dot{x}_0\}$ is given by:

$$\Gamma(x(t)) = \frac{(v + \delta_{\dot{x}} - q_1(x_0)^T \dot{x}_0)e^{-\omega t} + \omega(\Gamma(x_0) + v + \delta_{\dot{x}})t + q_1(x_0)^T \dot{x}_0 t - (v + \delta_{\dot{x}})}{\omega} \tag{16a}$$

$$q_1(x)^T \dot{x}(t) = (q_1(x_0)^T \dot{x}_0 - v - \delta_{\dot{x}})e^{-\omega t} + \delta_{\dot{x}} + v \tag{16b}$$

In the *first* region, as $0 < \Gamma(x_0)$ and $q_1(x_0)^T \dot{x}_0 < \delta_{\dot{x}}$, (16a) is monotonically decreasing and (16b) is monotonically increasing. Hence, based on (16b), $q_1(x(t^*))^T \dot{x}(t^*) = \delta_{\dot{x}}$ at $t^* = -ln(\frac{v}{v + \delta_{\dot{x}} - q_1(x_0)^T \dot{x}_0})\omega^{-1}$. Given $q_1(x_0)^T \dot{x}_0 < \delta_{\dot{x}}$, substituting (5), (9) and t^* into (16a) yields:

$$q_1(x(t^*))^T x(t^*) = (-(\delta_{\dot{x}} + v)\ln(\frac{v}{v + \delta_{\dot{x}} - q_1(x_0)^T \dot{x}_0}) - \delta_{\dot{x}} + q_1(x_0)^T \dot{x}_0)\omega^{-1} + \Gamma(x_0) \tag{17}$$

As $-\frac{q_1(x_0)^T \dot{x}_0}{\Gamma(x_0)} \leq \omega$ and $0 < \frac{\delta_{\dot{x}} - q_1(x_0)^T \dot{x}_0}{e^1 - 1} < v$, $q_1(x(t^*))^T x(t^*)$ defined by (17) is lower bounded by positive value:

$$0 < \overbrace{\frac{\Gamma(x_0)\delta_{\dot{x}}}{q_1(x_0)^T \dot{x}_0}}^{0<} \left(\ln\left(\frac{v}{v + \delta_{\dot{x}} - q_1(x_0)^T \dot{x}_0} \right) + 1 \right) + \overbrace{\frac{\Gamma(x_0)v}{q_1(x_0)^T \dot{x}_0}}^{<0} \ln\left(\frac{v}{v + \delta_{\dot{x}} - q_1(x_0)^T \dot{x}_0} \right) \tag{18}$$
$$\leq q_1(x(t^*))^T x(t^*) < \Gamma(x_0)$$

Hence, the robot's normal velocity is $\delta_{\dot{x}}$ while $0 < \Gamma(x)$. Moreover, as $0 < \frac{dq_1(x)^T \dot{x}}{dt}$ at $q_1(x)^T \dot{x} = \delta_{\dot{x}}$, the robot moves toward the contact surface with $\delta_{\dot{x}} \leq q_1(x)^T \dot{x}$. To sum up, in all three regions, the proposed modulation function regulates the normal velocity of the robot such that the contact will be stable. ∎

C. Proof of Proposition 1

To prove this proposition, we need to study the worse scenario; namely when $\eta = \eta$. In this case, to achieve the stability at the impact, $q_1(x)^T \dot{x} = \delta_{\dot{x}}$ at $\Gamma(x) = \eta$. Hence, (17) should be lower bounded by η:

$$(-(\delta_{\dot{x}} + v)\ln(\frac{v}{v + \delta_{\dot{x}} - q_1(x_0)^T \dot{x}_0}) - \delta_{\dot{x}} + q_1(x_0)^T \dot{x}_0)\omega^{-1} + \Gamma(x) = \eta \tag{19}$$

The aforementioned Eq. (19) with respect to $\frac{\delta_{\dot{x}} - q_1(x_0)^T \dot{x}_0}{e^1 - 1} < v \leq -\delta_{\dot{x}}, 0 < \omega$ does not have a unique solution. Nevertheless, one of the many solutions is $v = -\delta_{\dot{x}}$ and $\omega = \frac{\delta_{\dot{x}} - q_1^T \dot{x}_0}{\Gamma(x_0) - \eta}$. This, based on our experience, results in an acceptable performance. ∎

REFERENCES

[1] Y.-B. Jia, M. T. Mason, and M. A. Erdmann, "Multiple impacts: A state transition diagram approach," *The Intern. Journal of Robotics Research*, vol. 32, no. 1, pp. 84–114, 2013.

[2] P. R. Pagilla and B. Yu, "A stable transition controller for constrained robots," *IEEE/ASME Transactions on Mechatronics*, vol. 6, no. 1, pp. 65–74, Mar 2001.

[3] J. K. Mills and D. M. Lokhorst, "Stability and control of robotic manipulators during contact/noncontact task transition," *IEEE Transactions on Robotics and Automation*, vol. 9, no. 3, pp. 335–345, 1993.

[4] J. K. Mills, "Manipulator transition to and from contact tasks: A discontinuous control approach," in *IEEE Intern. Conf. on Robotics and Automation*. IEEE, 1990, pp. 440–446.

[5] T.-J. Tarn, Y. Wu, N. Xi, and A. Isidori, "Force regulation and contact transition control," *IEEE Control Systems*, vol. 16, no. 1, pp. 32–40, 1996.

[6] D. J. F. Heck, A. Saccon, N. van de Wouw, and H. Nijmeijer, "Switched position-force tracking control of a manipulator interacting with a stiff environment," in *2015 American Control Conf. (ACC)*, July 2015, pp. 4832–4837.

[7] M. Tomizuka, "Contact transition control of nonlinear mechanical systems subject to a unilateral constraint," *Journal of dynamic systems, measurement, and control*, vol. 119, p. 749, 1997.

[8] K. Youcef-Toumi and D. A. Gutz, "Impact and force control," in *IEEE Intern. Conf. on Robotics and Automation*. IEEE, 1989, pp. 410–416.

[9] L. Roveda, G. Pallucca, N. Pedrocchi, F. Braghin, and L. M. Tosatti, "Iterative learning procedure with reinforcement for high-accuracy force tracking in robotized tasks," *IEEE Transactions on Industrial Informatics*, vol. PP, no. 99, pp. 1–1, 2017.

[10] L. Roveda, N. Iannacci, F. Vicentini, N. Pedrocchi, F. Braghin, and L. M. Tosatti, "Optimal impedance force-tracking control design with impact formulation for interaction tasks," *IEEE Robotics and Automation Letters*, vol. 1, no. 1, pp. 130–136, Jan 2016.

[11] F. Ferraguti, C. Secchi, and C. Fantuzzi, "A tank-based approach to impedance control with variable stiffness." in *IEEE Intern. Conf. on Control Automation (ICRA*, 2013, pp. 4948–4953.

[12] C. Schindlbeck and S. Haddadin, "Unified passivity-based cartesian force/impedance control for rigid and flexible joint robots via task-energy tanks," in *2015 IEEE International Conference on Robotics and Automation (ICRA)*, May 2015, pp. 440–447.

[13] E. Lee, J. Park, K. A. Loparo, C. B. Schrader, and P. H. Chang, "Bang-bang impact control using hybrid impedance/time-delay control," *IEEE/ASME Transactions on Mechatronics*, vol. 8, no. 2, pp. 272–277, June 2003.

[14] M. Jin, S. H. Kang, P. H. Chang, and E. Lee, "Nonlinear bang-bang impact control: A seamless control in all contact modes," in *Proceedings of the 2005 IEEE Intern. Conf. on Robotics and Automation*, April 2005, pp. 557–564.

[15] S. S. M. Salehian and A. Billard, "A dynamical-system-based approach for controlling robotic manipulators during noncontact/contact transitions," *IEEE Robotics and Automation Letters*, vol. 3, no. 4, pp. 2738–2745, Oct 2018.

[16] S. S. Mirrazavi Salehian, "Compliant control of uni/ multi- robotic arms with dynamical systems," p. 169, 2018.

[17] A. Escande, S. Miossec, M. Benallegue, and A. Kheddar, "A strictly convex hull for computing proximity distances with continuous gradients," *IEEE Transactions on Robotics*, vol. 30, no. 3, pp. 666–678, June 2014.

[18] S. S. M. Salehian, N. Figueroa, and A. Billard, "A unified framework for coordinated multi-arm motion planning," *The International Journal of Robotics Research*, vol. 0, no. 0, p. 0278364918765952, 0.